HHS Public Access

Author manuscript

Curr Biol. Author manuscript; available in PMC 2023 March 28.

Published in final edited form as:

Curr Biol. 2022 March 28; 32(6): 1429–1438.e6. doi:10.1016/j.cub.2022.03.017.

Chloride oscillation in pacemaker neurons regulates circadian rhythms through a chloride-sensing WNK kinase signaling cascade

Jeffrey N. Schellinger[1], **Qifei Sun**[1], **John M. Pleinis**[2], **Sung-Wan An**[3], **Jianrui Hu**[2], **Gaëlle Mercenne**[2], **Iris Titos**[2], **Chou-Long Huang**[3], **Adrian Rothenfluh**[2,4,5,6], **Aylin R. Rodan**[2,6,7,8,9,*]

[1]Department of Internal Medicine, Division of Nephrology, University of Texas Southwestern, Dallas, TX, 75390, USA

[2]Molecular Medicine Program, University of Utah, Salt Lake City, UT, 84112, USA

[3]Department of Internal Medicine, Division of Nephrology, University of Iowa Carver College of Medicine, Iowa City, Iowa, 52242, USA

[4]Department of Psychiatry, Huntsman Mental Health Institute, University of Utah, Salt Lake City, UT, 84108, USA

[5]Department of Neurobiology, University of Utah, Salt Lake City, UT, 84112, USA

[6]Department of Human Genetics, University of Utah, Salt Lake City, UT, 84112, USA

[7]Department of Internal Medicine, Division of Nephrology and Hypertension, University of Utah, Salt Lake City, UT, 84132, USA

[8]Medical Service, Veterans Affairs Salt Lake City Health Care System, Salt Lake City, UT, 84148, USA

[9]Lead Contact

SUMMARY

[*]Corresponding author: Aylin Rodan, MD, PhD, Molecular Medicine Program, Department of Internal Medicine, Division of Nephrology and Hypertension, University of Utah, 15 North 2030 East, Bldg. 533, Room 2420A, Salt Lake City, UT 84112, USA, Phone: 801-587-7929, Fax: 801-585-0701, aylin.rodan@hsc.utah.edu.

AUTHOR CONTRIBUTIONS

Conceptualization, A.R.R. Investigation, J.N.S., Q.S., J.M.P., and S.A. Formal Analysis, A.R.R. Resources, J.H. and G.M. Writing – Original Draft, A.R.R. Writing – Review & Editing, A.R.R., I.T. and A.R. Visualization, A.R.R. and I.T. Supervision, A.R.R. and C.L.H. Project Administration, A.R.R. Funding Acquisition, A.R.R., A.R. and C.L.H.

DECLARATION OF INTERESTS

The authors declare no competing interests.

INCLUSION AND DIVERSITY STATEMENT

One or more of the authors of this paper self-identifies as an underrepresented ethnic minority in science. One or more of the authors of this paper self-identifies as a member of the LGBTQ+ community. One of more of the authors of this paper self-identifies as living with a disability.

Central pacemaker neurons regulate circadian rhythms and undergo diurnal variation in electrical activity in mammals and flies[1,2]. Circadian variation in the intracellular chloride concentration of mammalian pacemaker neurons has been proposed to influence the response to GABAergic neurotransmission through $GABA_A$ receptor chloride channels[3]. However, results have been contradictory[4–9], and a recent study demonstrated circadian variation in pacemaker neuron chloride without an effect on GABA response[10]. Therefore, whether and how intracellular chloride regulates circadian rhythms remains controversial. Here, we demonstrate a signaling role for intracellular chloride in the *Drosophila* small ventral lateral (sLN_v) pacemaker neurons. In control flies, intracellular chloride increases in sLN_vs over the course of the morning. Chloride transport through sodium-potassium-2-chloride (NKCC) and potassium-chloride (KCC) cotransporters is a major determinant of intracellular chloride concentrations[11]. *Drosophila melanogaster* with loss-of-function mutations in the NKCC encoded by *Ncc69* have abnormally low intracellular chloride six hours after lights on, loss of morning anticipation, and a prolonged circadian period. Loss of *kcc*, which is expected to increase intracellular chloride, suppresses the long-period phenotype of *Ncc69* mutant flies. Activation of a chloride-inhibited kinase cascade, consisting of WNK (With No Lysine (K)) kinase and its downstream substrate, Fray, is necessary and sufficient to prolong period length. Fray activation of an inwardly rectifying potassium channel, Irk1, is also required for the long-period phenotype. These results indicate that the NKCC-dependent rise in intracellular chloride in *Drosophila* sLN_v pacemakers restrains WNK-Fray signaling and overactivation of an inwardly rectifying potassium channel to maintain normal circadian period length.

eTOC

Schellinger et al. demonstrate intracellular chloride oscillations in the *Drosophila* sLN_v central pacemaker neurons regulate morning anticipation and circadian period. Chloride has a signaling role via the chloride-inhibited WNK kinase, which controls activity of an inwardly rectifying potassium channel via the intermediary kinase, Fray.

Graphical Abstract

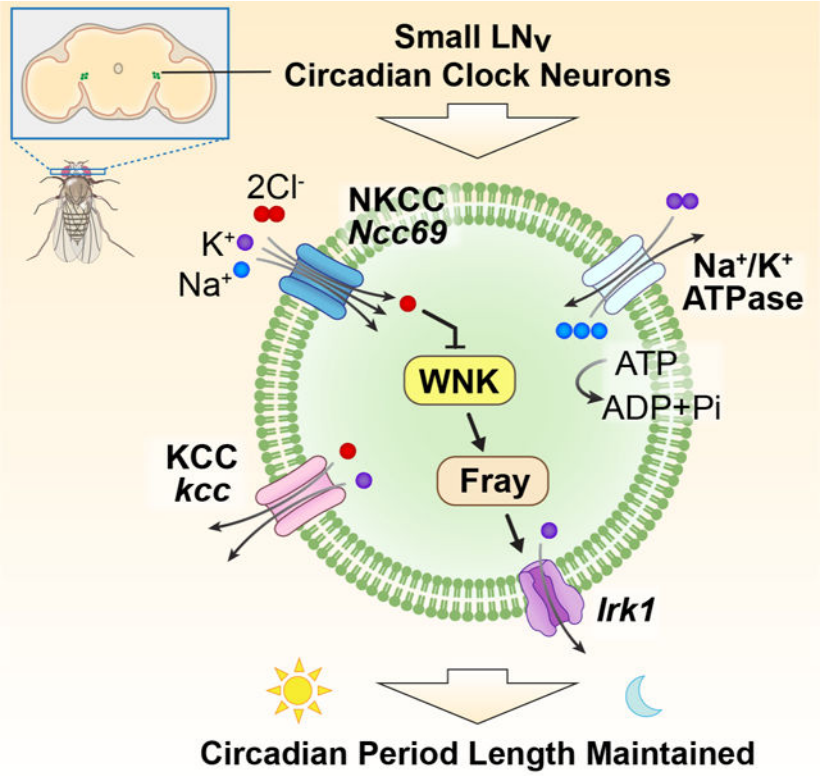

Keywords

circadian rhythm; chloride signalling; WNK; SPAK; Fray; Drosophila; potassium channel; SLC12; NKCC; KCC

RESULTS

Intracellular chloride increases in sLN$_v$ pacemakers during the morning in an NKCC-dependent manner

Na^+/K^+-ATPase activity results in low intracellular sodium and high intracellular potassium in most cells, generating an inward driving force for chloride through NKCCs and an outward driving force through KCCs[11]. These transporters are expressed in mammalian suprachiasmatic nucleus (SCN) clock neurons, where they determine intracellular chloride and the GABA reversal potential[4,5,7,9,10,12]. We used the transgenic sensor, ClopHensor, to measure intracellular chloride *ex vivo* in the small LN$_v$ neurons (sLN$_v$s), which are *Drosophila* central brain pacemaker cells[13]. sLN$_v$s from controls and from flies with strong loss-of-function mutations in *Ncc69*, which encodes an NKCC[14–16], were tested in parallel every 4 hours after lights on (ZT0). ClopHensor couples chloride-sensitive GFP to chloride-insensitive dsRed for ratiometric chloride measurement[17–20], with the cyan/red ratio inverse to chloride (Figure S1). Intracellular pH, which influences chloride measurement[17], was measured simultaneously, and was similar over time and between genotypes (Table S1). In controls, chloride rose during daytime, fell, and then rose again during nighttime (Figures 1A, S1D). Brains were exposed to light during dissection and imaging, which could

confound nighttime measurements. However, these results suggest that intracellular chloride varies in sLN_v pacemakers over the day/night cycle, as in the mammalian SCN[3,4,9,10].

Intracellular chloride appeared to increase from ZT2 to ZT6 in controls, but not in *Ncc69* mutants (Figures 1A, S1D). Since the ZT2 and ZT6 measurements were made in different neurons, we next performed repeated measurements in the same neurons at ZT2 and ZT6. Although the cyan/red ratios were slightly lower in this experiment, this experiment also showed that intracellular chloride rose from ZT2 to ZT6 in controls, but remained constant in *Ncc69* mutants, with lower chloride concentrations in *Ncc69* mutants compared to controls at ZT6 (Figures 1B, S1E). This indicates that intracellular chloride increases in sLN_vs over the course of the morning in an NKCC-dependent manner.

The *Ncc69* NKCC is required in sLN_v pacemakers for normal circadian behavior

To test the functional consequences of loss of NKCC activity on circadian rhythms, we examined locomotor activity in *Drosophila* activity monitors. sLN_vs regulate morning anticipation, the increase in locomotor activity that occurs prior to the onset of daylight in light-dark conditions[21–23]. Morning anticipation was abolished in *Ncc69* mutants, whereas evening anticipation, which is regulated by other clock neurons[21–23], was not affected (Figures 2A, B).

sLN_vs also regulate the free-running clock[24,25]. *Ncc69*^{r2} mutants had a prolonged period in constant darkness that was rescued by LN_v-specific expression of wild-type *Ncc69* (Figure 2C, D). Although the *pdf*-GAL4 driver is expressed in both small and large LN_v neurons (lLN_vs)[24], the latter have been implicated in sleep and arousal and likely do not contribute to the period-length phenotype[26–28].

Prolonged period was observed in *Ncc69*^{r2} homozygous mutants and in flies with *Ncc69*^{r2} over a deficiency deleting *Ncc69*, but not in heterozygotes (Figure 2C). LN_v morphology[24,29] was intact in *Ncc69*^{r2} mutants (Figure 2E). We observed weaker rhythmicity in *Ncc69*^{r2} homozygotes. This phenotype was not rescued by LN_v *Ncc69* expression, and was not observed in *Ncc69*^{r2}*/Df* (Table S3). Therefore, the reduced rhythm strength may be due to mutation in a different gene, or *Ncc69* activity outside the LN_vs, and was not pursued further. Roles for *Ncc69* have been demonstrated in glia, including decreased rhythmicity with glial *Ncc69* knockdown[14,30–32]. However, glial expression of wild-type *Ncc69* did not rescue the long-period phenotype or decreased rhythmicity of mutants (Table S3). Thus, *Ncc69* is specifically required in sLN_vs for the maintenance of normal circadian period.

Period lengthening in *Ncc69* mutants is due to low chloride activation of the WNK-Fray kinase cascade

We reasoned that decreasing KCC activity, which is expected to increase intracellular chloride, might reverse the *Ncc69* mutant phenotype. *kcc* heterozygous mutation or LN_v knockdown resulted in period lengths similar to, or slightly longer than, controls (Table S3). However, both maneuvers suppressed the long-period phenotype of *Ncc69* mutants (Figure 3A, B), further indicating that dysregulated intracellular chloride in sLN_vs drives the long-period phenotype of *Ncc69* mutants.

The *Ncc69* NKCC is activated by the *Drosophila* WNK-Fray kinase cascade, homologs of the WNK-SPAK/OSR1 (Ste20-related proline alanine rich kinase/oxidative stress response) kinases that activate mammalian NKCCs[33,34]. In addition, chloride inhibits WNK signaling through direct effects on mammalian and *Drosophila* WNKs[19,35,36]. We first tested the hypothesis that LN_v loss of *WNK* or *Fray* would phenocopy the *Ncc69* loss-of-function phenotype, i.e. circadian period lengthening, due to loss of positive regulation by the kinases. We observed only a slight increase (9–36 minutes) in period length in *WNK* knockdown flies, and there was no effect of *Fray* knockdown (Table S4), suggesting that *WNK* and *Fray* do not act upstream of *Ncc69* in circadian period regulation.

The prolonged circadian period of *Ncc69* mutants could also be due to decreased late-morning sLN_v intracellular chloride and excess WNK-Fray activation. Consistent with this hypothesis, LN_v knockdown of either *WNK* (Figure 3C) or *Fray* (Figure 3D) suppressed the $Ncc69^{r2}$ long-period phenotype. Conversely, LN_v overexpression of the Cl^--insensitive WNK^{L421F} mutant[19,35] caused period lengthening, phenocopying *Ncc69* mutants (Figure 3E). Overexpressing wild-type *WNK* had no effect, emphasizing the importance of chloride regulation of WNK in circadian period regulation (Figure 3E). Mammalian WNK3 is expressed in SCN pacemaker neurons[12]. LN_v overexpression of chloride-insensitive, but not wild-type, human $WNK3^{L295F}$ also resulted in circadian period lengthening, indicating phylogenetically conserved effects of this signaling pathway (Figure 3F and Table S3). Thus, sLN_v loss of WNK chloride inhibition is sufficient to prolong period length.

WNK kinases phosphorylate the T-loop threonine of SPAK/OSR1 kinases to activate them[37,38]. Mutation of the Fray T-loop threonine, T206, to a phosphomimicking glutamate results in WNK-independent Fray activation, and rescues the ion transport defect in renal tubules with *Drosophila WNK* knockdown[39]. The Fray D185A mutation abolishes kinase activity[39]. LN_v overexpression of $Fray^{T206E}$ increased period length in a kinase activity-dependent manner, mirroring the phenotype of loss of *Ncc69* or expression of chloride-insensitive WNK (Figure 3G, Table S3). Thus, loss of *Ncc69* results in failure of intracellular chloride to rise during the morning hours, and, as a consequence, WNK and Fray overactivation, initiating a signaling cascade that prolongs circadian period.

Fray activates the inwardly rectifying potassium channel Irk1 to prolong circadian period

To identify possible Fray targets required for circadian period prolongation, we queried the *Drosophila* proteome for putative Fray RFXV/I binding motifs[40] and identified 127 candidates using an optimized motif (see Methods) (Data S1A). We pursued the inwardly rectifying potassium channel, Irk1 (also known as Ir), for three reasons. First, LN_v *Irk1* knockdown affects circadian period[41]. Second, *Irk1* transcript is highly enriched in LN_vs, and exhibits transcriptional and translational cycling[42,43]. Third, the mammalian Fray homolog, OSR1, regulates mammalian inwardly rectifying potassium channels containing RFXV-related motifs (i.e., RXFXV)[44].

To examine whether Fray regulates Irk1 channel activity, we performed whole-cell patch clamp recordings of S2-R+ cultured *Drosophila* cells transfected with Irk1, with or without $Fray^{T206E}$ co-expression from a multi-cistronic plasmid. Irk1 activity was determined from barium-sensitive currents (Figure S2). $Fray^{T206E}$ expression increased Irk1 channel activity.

Mutation of the putative Irk1 Fray-binding RFXV motif to RFXA ($Irk1^{V306A}$) decreased channel activity relative to wild-type Irk1 in the absence of co-transfected $Fray^{T206E}$. Fray is endogenously expressed in S2-R+ cells[45], so this could represent decreased stimulation by endogenous Fray, although we cannot rule out direct effects of the mutation on the channel. The Irk1 RFXA mutation also blunted stimulation by $Fray^{T206E}$, with no significant difference in Irk1 current density with or without $Fray^{T206E}$ co-expression at a holding potential of −150 mV (Figure 4A, B). Together, these results indicate a stimulatory effect of $Fray^{T206E}$ on wild-type, but not RFXA mutant Irk1.

We next assessed the *in vivo* role of Fray stimulation of Irk1. We designed $Irk1^{WT}$ and $Irk1^{V306A}$ transgenes to be resistant to a previously-validated short hairpin Irk1 RNAi[46], allowing replacement of endogenous pacemaker neuron Irk1 with either the wild-type or V306A mutant. LN_v *Irk1* knockdown and replacement with either $Irk1^{WT}$ or $Irk1^{V306A}$ had no effect on period length (Figure 4C), consistent with the lack of phenotype with *Fray* knockdown (Table S4). Expressing $Fray^{T206E}$ in the pacemaker neurons increased period length in wild-type flies and in flies with endogenous Irk1 replaced with $Irk1^{WT}$, while replacement of Irk1 with $Irk1^{V306A}$ suppressed the long-period phenotype (Figure 4C). This suggests that Fray stimulation of Irk1 is required for the long-period phenotype observed with loss of *Ncc69* and activation of the WNK-Fray kinase cascade.

DISCUSSION

Intracellular chloride oscillates in central pacemaker neurons of the mammalian SCN[3,4,9,10], but the functional significance of this oscillation has remained unclear. Here, we demonstrate an NKCC-dependent increase in intracellular chloride in *Drosophila* sLN_v pacemaker neurons over the course of the morning, which constrains activity of the chloride-sensitive WNK kinase, its downstream substrate, Fray, and an inwardly rectifying potassium channel, Irk1, to maintain normal circadian periodicity. Loss of the Ncc69 NKCC in LN_v pacemaker neurons results in loss of morning anticipation and lengthening of the circadian period in free-running conditions. Our observations are consistent with studies in the SCN implicating NKCC in the determination of intracellular chloride in mammalian pacemaker neurons[4,5,7,9,10,12], and connects intracellular chloride to behavioral circadian phenotypes.

Diurnal variations in intracellular chloride have been proposed to influence the effect of GABAergic neurotransmission on clock neurons in mammals[3–9], but a recent study challenged this idea[10]. Existing data indicate a minor role for sLN_v ligand-gated chloride channels in the regulation of circadian period[27,28,47–49]. Rather, we demonstrate a signaling role for chloride in sLN_vs, via inhibition of WNK-Fray signaling. As chloride-sensitive kinases, WNKs are poised to interpret changes in intracellular chloride and initiate downstream signal transduction cascades[35,50,51]. This has been studied in transepithelial ion transport in *Drosophila* and mammalian renal epithelia[19,52,53], as well as in the clearance of apoptotic corpses[54]. Our findings further extend this concept to circadian pacemaker neurons.

KCC and another cation-chloride cotransporter, encoded by the *NKCC* gene, have been linked to the electrophysiological response to GABA in lLN_vs, which express $GABA_A$

receptor chloride channels[27,28,55] (Eick et al, this issue). The transport activity of the *NKCC*-encoded transporter has not been characterized, but may differ from the Ncc69 NKCC, as suggested by sequence differences and the transport activity of an *Aedes aegypti* ortholog[56,57]. Expression of *Ncc69* and *NKCC* may also differ. Consistent with this idea, broad clock neuron knockout of *NKCC* has no effect on morning anticipation or period length, but leads to abnormal rhythmicity in constant light, as does *NKCC* overexpression or loss or gain of *kcc*[55] (Eick et al, this issue). Thus, intracellular chloride likely affects clock neurons both by affecting the driving force for chloride through neurotransmitter-gated chloride channels, and via inhibition of WNK-Fray signaling. Interestingly, knocking down *WNK* and *Fray* broadly in clock neurons phenocopies loss of *kcc* and *NKCC* in the same neurons (Eick et al., this issue), suggesting that WNK and Fray act in their usual regulatory roles upstream of the transporters in this case, and further highlighting distinct actions of this pathway in different subpopulations of *Drosophila* clock neurons.

Pacemaker neurons in flies and mammals undergo cell-autonomous, molecular clock-controlled circadian variation in electrical activity[1,2,13,58–60], and altering the excitability of the LN_v pacemakers disrupts circadian rhythms[41,61–65]. Two voltage-gated potassium channels have been implicated in LN_v neuron electrical oscillations[66], and a sodium leak current and potassium channels contribute to the day/night cycling of resting membrane potential in *Drosophila* dorsal clock neurons[67]. Because inwardly rectifying potassium channels play an important role in determining cellular membrane potential[68], which is thought to be a determinant of circadian variation in electrical activity[1,2], chloride regulation of Irk1 activity could also contribute to the diurnal variation in sLN_v excitability. Specifically, Irk1 activation at ZT6 due to low intracellular chloride and activation of the WNK-Fray pathway in *Ncc69* mutants may disrupt the usual circadian pattern of membrane depolarization and hyperpolarization in sLN_vs[69], thereby altering period length.

Could intracellular chloride play a signaling role in SCN pacemaker neurons? NKCC1, KCCs and WNK3 are expressed in the rat SCN[12]. The repertoire of ion channels regulating pacemaker neuron excitability is complex and incompletely understood, but large-conductance Ca^{2+}-activated potassium channels have been implicated, and are regulated by mammalian WNKs[2,70–75]. Whether oscillating intracellular chloride observed in SCN neurons regulates these or other ion channels modulating pacemaker neuron electrical properties will be of interest for future investigation.

STAR METHODS

RESOURCE AVAILABILITY

Lead Contact—Further information and requests for resources and reagents should be directed to and will be fulfilled by the lead contact, Aylin Rodan (aylin.rodan@hsc.utah.edu).

Materials Availability—All materials generated for this study, such as plasmids and fly lines, are available upon request from the Lead Contact.

Data and Code Availability—All data reported in this paper will be shared by the lead contact upon request. This paper does not report original code. Any additional information required to reanalyze the data reported in this paper is available from the lead contact upon request.

EXPERIMENTAL MODEL AND SUBJECT DETAILS

Drosophila* Strains and Fly Husbandry—Drosophila melanogaster* strains used are shown in the Key Resources Table and the genotypes used for each experiment are shown in Table S2. *w; pdf*-GAL4, *w*; UAS-WNK^{RNAi}, *w*; UAS-Fray^{RNAi}, *w*; UAS-Irk1^{RNAi}, *w;* UAS-kcc^{RNAi}, *w;* UAS-Fray^{T206E}, *w;* UAS-WNK^{WT}, *w*; UAS-WNK^{L421F}, *w;* UAS-WNK3^{WT}, *w;* UAS-WNK3^{L295F}, *w;* UAS-Fray^{D185A,T206E} and *w;* UAS-dcr-2 were outcrossed for 5 generations to *wBerlin*, which was also used for generating heterozygous controls (e.g., *w; pdf*-GAL4/+). Except for *w;* UAS-Fray^{RNAi} (Vienna), and *w;* UAS-kcc^{RNAi}, knockdown of the targeted genes has previously been validated by qRT-PCR, as referenced in the Key Resources Table. Recombinant chromosomes and combinations of transgenes were generated by standard genetic techniques. Generation of new transgenic strains is described below. Flies were reared on a standard cornmeal-yeast-molasses medium prepared in a central kitchen at UT Southwestern or the University of Utah. Flies were reared at room temperature (22–23 °C) or at 25 °C. Young adult (<2 week old) male flies were used in all assays. Males were used to avoid female egg-laying and the emergence of larvae in *Drosophila* activity monitors.

Cell lines—S2-R+ cultured *Drosophila* cells were obtained from Helmut Krämer (UT Southwestern) or the *Drosophila* Genomics Resource Center (stock #150) and cultured at 25 °C in Schneider's medium (Thermo Fisher Cat #21720001) with 10% FBS (Thermo Fisher Cat #10082139). S2-R+ cells are male[76]. Cells were not authenticated prior to use.

METHOD DETAILS

Generation of *Drosophila* transgenics—The open reading frame encoding Fray^{D185A,T206E} was recombined from pENTR-Fray^{D185A,T206E} [39] into the pUASg.attB Gateway-compatible destination vector, obtained from Johannes Bischof and Konrad Basler (Zürich, Switzerland)[77], using LR Clonase II (Thermo Fisher Cat #11791020). After sequence confirmation, midiprep DNA was injected into stock #24481 (*y*^{1}*M{vas-int.Dm}ZH-2A w**; *M{3xP3-RFP.attP′}ZH-22A*) by Rainbow Transgenic Flies (Camarillo, CA). Single male transformants were isolated by the presence of 'mini white' and confirmation of the UAS-transgene was performed by PCR with sequence-specific primers.

A plasmid (FI16807, stock #1644763) containing the open reading frame of *Irk1* was obtained from the *Drosophila* Genomics Resource Center (Indiana University, Bloomington, IN). The open reading frame was PCR-amplified (Phusion high-fidelity DNA polymerase, New England Biolabs Cat #M0530) using primers Irk1-F and Irk1-R (primers and plasmids are listed in the Key Resources Table and Table S6). After gel extraction (Qiagen QIAquick Cat #28104), the PCR product was cloned into pENTR using the pENTR/D-TOPO cloning kit (Thermo Fisher Cat #K240020) and the sequence confirmed by Sanger sequencing. Next, a mutation was introduced into pENTR-Irk1^{WT} to generate a mutation in the putative Fray-

binding motif, in which Val 306 in the "RFXV" motif is mutated to Ala. The corresponding "GTG" was mutated to "GCG" using QuikChange II XL (Agilent Cat #200521) and primers Irk1-V306A-F and Irk1-V306A-R to generate pENTR-Irk1^{V306A}. Next, mutations were introduced into pENTR-Irk1^{WT} and pENTR-Irk1^{V306A} to render the transgenes resistant to knockdown by co-expression of the Irk1 RNAi. Every third nucleotide in the twenty base pairs targeted by the RNAi was mutated in order to introduce five silent mutations (i.e., CTAAAGGAACGCTTC was mutated to CTGAAAGAGCGTTTT), using QuikChange II XL (Agilent Cat #200521) and primers Irk1-RR-F and Irk1-RR-R. The resulting plasmids were called pENTR-Irk1^{WT-RR} and pENTR-Irk1$^{V306A-RR}$. Irk1 sequences in all plasmids were confirmed by Sanger sequencing. The open reading frames of Irk1^{WT-RR} and Irk1$^{V306A-RR}$ were then recombined into pUASg.attB using LR Clonase II (Thermo Fisher Cat #11791020) to generate pUASg.attB-Irk1^{WT-RR} and pUASg.attB-Irk1$^{V306A-RR}$. Midiprep DNA was injected into stock #24483 (*M{vas-int.Dm}ZH-2A, M{3xP3-RFP.attP}ZH- 51D*), transformants isolated, and UAS-transgenes confirmed as above.

Circadian rhythm analysis—Male flies were collected within 72 hours of eclosion and kept on standard food for 3–5 days in a 12-hour oscillating light/dark incubator. After the entrainment period, individual flies were placed into 5 mm diameter glass cuvettes with standard medium at one end and a tissue plug at the other, allowing the flies free movement throughout the cuvette. Beam breaking by locomotor activity was recorded in 30 minute increments (bins) using *Drosophila* Activity Monitors (TriKinetics) in constant darkness over a period of 7 days. Activity data were then analyzed using FAASx software (Paris-Saclay Institute of Neuroscience). Cycle p analyses provided period length (tau) and rhythmic strength (power) for individual flies. Settings used were: Minimum period peak power 20, Minimum period peak width 0200. Output was restricted to flies with period lengths of 26 hours ± 10 hours (minimum tau 16, maximum 36). Flies that did not survive the full 7 days (168 hours) or were arrhythmic (power less than 20) were not included in tau analysis.

For experiments in light:dark (LD) conditions, individual flies were loaded into cuvettes 24–72 hours after eclosion and remained in the Drosophila Activity Monitors in LD at room temperature (~22–23 °C) for 6 days. Data from the final 3 days, after 3 days of entrainment, was used for analysis. Morning and evening anticipation index was calculated according to the methods of Schlichting *et al.*[78]: morning anticipation index = sum of activity ZT21-ZT0/sum of activity ZT18-ZT0, and evening anticipation index = sum of activity ZT9-ZT12/sum of activity ZT6 – ZT12.

For the Irk1 experiment, analysis was performed in ClockLab version 6 (Actimetrics, Wilmette, IL), using the chi squared periodogram function. Settings used were: Start Day 1, End Day 9, type chi squared, start 16 hours (minimum tau), end 36 hours (maximum tau), significance 0.01. In order to classify rhythmic strength, cutoffs were determined by assaying *wBerlin* control flies. Flies that did not survive the full 8 days or were arrhythmic (power less than 2500) were not included in tau analysis.

PDF neuron immunohistochemistry—Brains were dissected from adult flies in PBS (phosphate-buffered saline, in mM: 137 NaCl, 2.7 KCl, 8.1 Na_2HPO_4, 1.5 KH_2PO_4, pH 7.3–7.4) and fixed for 20–40 minutes in 4% formaldehyde. Brains were then rinsed in PBS, followed by PBT (PBS+0.3% Triton X-100) 4–5 times. Brains were incubated in mouse anti-PDF (PDF C7 from Developmental Studies Hybridoma Bank, Iowa City, IA[79]), 1:800 in 10% normal goat serum in PBT, overnight at 4°C, then rinsed 4–5 times in PBT and 2–3 times in PBS. Brains were then incubated in 1:800 goat anti-mouse Alexa Fluor 488 secondary antibody (Thermo Fisher Scientific Cat #A-11001) overnight, rinsed in PBT and PBS, and then mounted in 80% glycerol in PBS. Imaging was performed using a Zeiss LSM510 confocal microscope.

Measurement of intracellular Cl^-—The transgenic sensor ClopHensor, which contains a chloride-sensitive enhanced GFP variant (E^2GFP, carrying a T203Y mutation) coupled to a chloride-insensitive monomeric dsRed, allows ratiometric measurement of chloride based on emission after excitation at 458 nm (chloride-sensitive) and 543 nm (chloride-insensitive). ClopHensor is less prone to bleaching compared to other chloride sensors, and provides stable and long-lasting readouts of intracellular chloride, making it suitable for the measurements over time described below. Simultaneous measurement of pH can be accomplished due to the pH-dependent E^2GFP signal after excitation at 488 nm and the pH-independent E^2GFP signal after excitation at 458 nm, providing a ratiometric measurement of pH[17,18].

pH calibration: pcDNA3-ClopHensor (Addgene plasmid #25938) was cut with HindIII (New England Biolabs Cat #R3104) and NotI (New England Biolabs Cat #R3189) and the resulting product ligated into pIB (Thermo Fisher Cat #V802001) to generate pIB-ClopHensor. pIB-ClopHensor was transiently transfected into S2-R+ cultured *Drosophila* cells obtained from Helmut Krämer (UT Southwestern) using CellFectin reagent (Thermo Fisher Cat #10362100). 48 hours after transfection, cells were bathed in pH-varied solution containing: 38 mM Na gluconate, 100 mM K gluconate, 0.6 mM $MgSO_4$, 20 mM HEPES (varied pH), 10 μM tributyltinchloride (Sigma Cat #T50202), 5 μM nigericin (Thermo Fisher Cat #N1495), 5 μM carbonyl cyanide 3-chlorophenylhydrazone (Sigma Cat # C2759) and 5 μM valinomycin (Sigma Cat # V0627). After equilibration for at least 1 hour, cells were imaged using a Zeiss LSM510 confocal microscope, with excitation at 488 nm (green emission) and 458 nm (cyan emission). Individual cells (19–25 cells for each pH) were then outlined and pixel intensity measured using ImageJ without image manipulation. The ratios of green/cyan vs. pH were entered into GraphPad Prism, and a sigmoidal curve interpolated using the function “sigmoidal, 4PL, X is log(concentration).” This provided the values for the following equation, used to calculate intracellular pH (pH_i) in the pacemaker neurons[18]:

$$pH_i = pK_a - \frac{1}{p} * \log\left(\frac{B2 - B1}{R_{pH} - B1} - 1\right)$$

where R_{pH} is the experimentally derived green/cyan ratio, pK_a = 7.254, p = power (Hill slope, 1.668), and $B1$ (0.2603) and $B2$ (1.915) are the minimum and maximum asymptotic values of R_{pH}.

Cl^- calibration: Brains expressing ClopHensor in the pacemaker neurons (*w/Y; pdf*-GAL4 UAS-ClopHensor c202) were dissected from 3–5 day old flies in *Drosophila* saline, consisting of (in mM): NaCl 117.5, KCl 20, $CaCl_2$ 2, $MgCl_2$ 8.5, $NaHCO_3$ 10.2, NaH_2PO_4 4.3, HEPES 15, and glucose 20, pH 7.0. Brains were attached to the bottom of 35 mm glass bottom dishes with 14 mm microwell/#1.5 cover glass (Cellvis) coated with poly-lysine, and the solution exchanged to the chloride calibration solution, consisting of (in mM): 100 mM Na-Cl/gluconate, 50 mM K-Cl/gluconate, 2 mM Ca-Cl/gluconate, 8.5 mM Mg-Cl/gluconate, 20 mM glucose, 15 mM HEPES pH 7.1, 10 μM tributyltinchloride, 5 μM nigericin, 5 μM carbonyl cyanide 3-chlorophenylhydrazone and 5 μM valinomycin. Cl/gluconate anions were adjusted to achieve varying chloride concentrations. After 1 hour equilibration, brains were imaged using a Zeiss LSM510 confocal microscope, with excitation at 543 nm (red emission) and 458 nm (cyan emission). Individual neuron cell bodies (10 per Cl^- concentration, from multiple brains) were outlined and pixel intensity measured in ImageJ without image manipulation. The ratios of cyan/red vs Cl^- were entered into GraphPad Prism, and a sigmoidal curve interpolated using the function “sigmoidal, 4PL, X is log(concentration).” This provided the values for the following equation, used to calculate intracellular Cl^- ($[Cl^-]_i$)[18]:

$$[Cl^-]_i = K_d * \left(\frac{A1 - A2}{R_{Cl} - A2} - 1\right)^{\frac{1}{p}}$$

where R_{Cl} is the experimentally derived cyan/red ratio, K_d = 53.49, p = power (set to 1 per methods of[18]), and $A1$ (1.538) and $A2$ (0.597) are the maximum and minimum asymptotic values of R_{Cl}.

Measurement of R_{pH} and R_{Cl}: Male flies were entrained in 12:12 LD conditions at room temperature (~22–23 °C) for 4 days. Brains expressing ClopHensor in the pacemaker neurons were removed from the incubator at specific ZT times (time after lights on), after which they were exposed to ambient daytime light, and dissected in the following solution, adapted from solutions used for two-photon calcium imaging of fly brain neuronal activity[80]: in mM, NaCl 108, KCl 5, $CaCl_2$ 2, $MgCl_2$ 8.2, $NaHCO_3$ 4, NaH_2PO_4 1, trehalose 5, sucrose 10, HEPES 5, pH 7.5. Dissected brains were attached to the bottom of 35 mm glass bottom dishes with 14 mm microwell/#1.5 cover glass (Cellvis) coated with poly-lysine, and then bathed in the above solution for about 60 minutes prior to imaging using a Zeiss LSM510 confocal microscope, with excitation at 543 nm (red emission), 488 nm (green emission), and 458 nm (cyan emission). Individual sLN_v neuronal cell bodies (distinguished from lLN_v neurons based on position and size) were outlined in ImageJ and pixel intensity captured for each emission channel. The ratios of green/cyan and cyan/red were used to calculate pH and Cl^- as described above. pH and Cl^- were measured for each individual neuron. For practical reasons, measurements on brains removed at different ZT times across 24 hours were performed on separate days, but control and *Ncc69* mutant brains were always tested in parallel. In order to specifically examine the effect of time of day in each genotype, we performed paired measurements in the same brains, as we performed previously in Malpighian tubule epithelial cells[19]. Flies were removed from the incubator at ZT2, and brains were dissected and imaged as above. The dishes were then

sealed with parafilm to prevent evaporation and returned to the incubator (in which lights were still on) for four hours. The same brains were re-imaged 4 hours later.

Proteome-wide search for Fray binding motifs—The *Drosophila* proteome was searched for putative Fray binding motifs, using the methods of Delpire and Gagnon[40]. First, the NCBI protein database was searched for *Drosophila melanogaster* and results were saved to a FASTA text file. Duplicate results and results from organisms other than *D. melanogaster* were eliminated. This list was then searched for two motifs. One motif, [S/G/V]RFx[V/I]xx[I/V/T/S], was derived from Delpire and Gagnon[40], and is called the "Gagnon motif" in (Data S1B). However, this screen failed to identify Ncc69, which we have previously validated as a Fray target[39]. It also failed to identify KCC, which is a validated mammalian SPAK/OSR1 target[81–84]. We therefore performed sequence alignment of the *Drosophila* homologs of three of the best-known families of mammalian SPAK/OSR-interacting proteins: WNKs, NKCCs/NCC, and KCCs (*Drosophila* WNK, Ncc69, and *Drosophila* KCC, respectively). From this we derived a second motif, referred to as the "*Drosophila* motif" (Data S1A): [D/E/N/Q/S/T/Y]RFx[V/I]xxxx[D/E/G/P]. A second list of proteins was generated using this motif.

Patch clamp analysis of Irk1

Generation of plasmids for S2 cell expression: To generate plasmids for cellular expression of $Irk1^{WT}$ and $Irk1^{V306A}$, with or without $Fray^{T206E}$ co-expression, the $Irk1^{WT}$ and $Irk1^{V306A}$ open reading frames were amplified from pENTR-$Irk1^{WT}$ or pENTR-$Irk1^{V306A}$ by PCR (Phusion high-fidelity DNA polymerase, New England Biolabs Cat #M0530). Primers pAc5-Irk1-F and pAc5-Irk1-R included additional sequence for subsequent Gibson assembly cloning into the multi-cistronic vector, pAc5 STABLE2 Neo (Addgene Cat #32426[85]), which uses T2A sequences to generate multiple polypeptides off of a single transcript, and also contains a GFP cassette. The pAc5 plasmid backbone was PCR-amplified using primers pAc5-F and pAc5-R. The products were then assembled using NEBuilder HiFi DNA Assembly (New England Biolabs Cat #E2621) to generate plasmids pAc5-$Irk1^{WT}$ and pAc5-$Irk1^{V306A}$. Irk1 inserts were confirmed by Sanger sequencing. Then, the open reading frame encoding $Fray^{T206E}$ was amplified from an existing pENTR-$Fray^{T206E}$ plasmid[39], using primers pAc5-Fray-F and pAc5-Fray-R, and the pAc5-$Irk1^{WT}$ or pAc5-$Irk1^{V306A}$ plasmid backbones were amplified using primers pAc5-Irk1-Fray-F and pAc5-Irk1-Fray-R. Using this strategy, the Neo^{R} cassette was replaced by the open reading frame encoding $Fray^{T206E}$, while the GFP cassette was retained to allow for identification of successfully transfected cells. After Gibson assembly, inserts were confirmed by Sanger sequencing. However, the Irk1 ORF contained a stop codon at the end, which would prevent expression of the downstream $Fray^{T206E}$. The stop codon was removed using QuikChange II XL (Agilent Cat #200521) and primers Irk1-TGA-F and Irk1-TGA-R.

Patch clamp of Irk1-expressing S2-R+ cells: S2-R+ *Drosophila* cultured cells were obtained from the *Drosophila* Genomics Resource Center (stock #150) and cultured at 25 °C in Schneider's medium (Thermo Fisher Cat #21720001) with 10% FBS (Thermo Fisher Cat #10082139). Cells were seeded at a density of 1.7×10^6 cells/ml in 12 well dishes for 24 hours and resuspended in serum-free medium prior to transfection. Cells were transfected

with 1 μg plasmid DNA (pAc5-Irk1^{WT}, pAc5-Irk1^{V306A}, pAc5-Irk1^{WT}-Fray^{T206E}, or pAc5-Irk1^{V306A}-Fray^{T206E}) in 100 μL Opti-MEM (Thermo Fisher Cat #31985088) using 2 μL of TransIT-Insect transfection reagent (Mirus Bio Cat #6104). Medium was replaced with serum-containing medium 5 hours after transfection. Irk1 activity was measured in GFP+ cells 48–72 hours after transfection. Cells were harvested by centrifugation and resuspended in fresh medium. They were then plated on cover slips coated with poly-L-lysine (Sigma P8920). Ruptured whole cell recordings were performed at room temperature in a bath solution containing (in mM) 135 KCl, 1 $MgCl_2$, 2 $CaCl_2$, 15 glucose, 10 HEPES, 15 sucrose, pH 7.4 with Tris. Patch pipettes were pulled from borosilicate glass capillaries (Sutter Instruments) and heat-polished to give input resistances of 2–3 megaohms. The pipette recording solution contained (in mM) 135 KCl, 1 $MgCl_2$, 2 ATP-Mg, 0.1 GTP-Na, 5 EGTA, 10 HEPES, pH 7.2 with Tris. Cells were held at 0 mV and stimulated for 400 ms with step pulses from −150 mV to +90 mV with 20 mV steps. Currents were recorded with an Axopatch 200B patch-clamp amplifier and Pulse software (Molecular Devices, Sunnyvale, CA). 0.5 mM Ba^{2+} inhibited inward currents with 135 mM K^+, and washing with Ba^{2+}-free 135 mM K^+ recovered the currents. Ba^{2+}-sensitive current was therefore analyzed. Data acquisition and analysis were performed using pClamp v.9.2 (Molecular Devices).

QUANTIFICATION AND STATISTICAL ANALYSIS

Statistical testing was performed using GraphPad Prism, version 9. Data sets were analyzed for normality using the D'Agostino & Pearson normality test. Normally distributed data were compared using t-test or ANOVA and non-normally distributed data were compared using Mann-Whitney or Kruskal-Wallis test. Multiple comparisons testing was performed as indicated in the figure legends or Table S3. $p<0.05$ was considered statistically significant. Number of flies or cells examined and statistical parameters are indicated in the figure legends or Tables S1–S4.

Supplementary Material

Refer to Web version on PubMed Central for supplementary material.

ACKNOWLEDGEMENTS

The authors would like to thank Billy Leiserson, Michael Rosbash and Daria Hekmat-Scafe for fly lines, Johannes Bischof and Konrad Basler for plasmids, Helmut Krämer for S2-R+ cells, and Diana Lim for assistance with figures. Stocks obtained from the Bloomington *Drosophila* Stock Center (NIH P40OD018537) and the Vienna Drosophila Resource Center were used in this study. Plasmids and S2-R+ cells were obtained from the *Drosophila* Genomics Research Center (Indiana University, Bloomington, IN, supported by NIH grant 2P40OD010949). The PDF C7 antibody, developed by Justin Blau (New York University), was obtained from the Developmental Studies Hybridoma Bank, created by the NICHD of the NIH and maintained at The University of Iowa, Department of Biology, Iowa City, IA 52242. This work was supported by the National Institutes of Health: DK091316, DK106350 and DK110358 to A.R.R.; DK111542 to C.L.H.; and AA019526, AA026818 and DA049635 to A.R.

REFERENCES

1. Allen CN, Nitabach MN, and Colwell CS (2017). Membrane Currents, Gene Expression, and Circadian Clocks. Csh Perspect Biol 9, a027714.
2. Harvey JRM, Plante AE, and Meredith AL (2020). Ion Channels Controlling Circadian Rhythms in Suprachiasmatic Nucleus Excitability. Physiol Rev 100, 1415–1454. [PubMed: 32163720]

3. Wagner S, Castel M, Gainer H, and Yarom Y (1997). GABA in the mammalian suprachiasmatic nucleus and its role in diurnal rhythmicity. Nature 387, 598–603. [PubMed: 9177347]
4. Alamilla J, Perez-Burgos A, Quinto D, and Aguilar-Roblero R (2014). Circadian Modulation of the Cl – Equilibrium Potential in the Rat Suprachiasmatic Nuclei. Biomed Res Int 2014, 1–15.
5. Choi HJ, Lee CJ, Schroeder A, Kim YS, Jung SH, Kim JS, Kim DY, Son EJ, Han HC, Hong SK, et al. (2008). Excitatory actions of GABA in the suprachiasmatic nucleus. J Neurosci Official J Soc Neurosci 28, 5450–9.
6. Gribkoff VK, Pieschl RL, Wisialowski TA, Park WK, Strecker GJ, Jeu M.T.G. de, Pennartz CMA, and Dudek FE (1999). A Reexamination of the Role of GABA in the Mammalian Suprachiasmatic Nucleus. J Biol Rhythm 14, 126–130.
7. Irwin RP, and Allen CN (2009). GABAergic signaling induces divergent neuronal Ca 2+ responses in the suprachiasmatic nucleus network. Eur J Neurosci 30, 1462–1475. [PubMed: 19821838]
8. Jeu MD, and Pennartz C (2002). Circadian Modulation of GABA Function in the Rat Suprachiasmatic Nucleus: Excitatory Effects During the Night Phase. J Neurophysiol 87, 834–844. [PubMed: 11826050]
9. Shimura M, Akaike N, and Harata N (2002). Circadian rhythm in intracellular Cl – activity of acutely dissociated neurons of suprachiasmatic nucleus. Am J Physiol-cell Ph 282, C366–C373.
10. Klett NJ, and Allen CN (2017). Intracellular Chloride Regulation in AVP+ and VIP+ Neurons of the Suprachiasmatic Nucleus. Sci Rep-uk 7, 10226.
11. Kaila K, Price TJ, Payne JA, Puskarjov M, and Voipio J (2014). Cation-chloride cotransporters in neuronal development, plasticity and disease. Nat Rev Neurosci 15, 637–654. [PubMed: 25234263]
12. Belenky MA, Sollars PJ, Mount DB, Alper SL, Yarom Y, and Pickard GE (2010). Cell-type specific distribution of chloride transporters in the rat suprachiasmatic nucleus. Neuroscience 165, 1519–1537. [PubMed: 19932740]
13. King AN, and Sehgal A (2020). Molecular and circuit mechanisms mediating circadian clock output in the Drosophila brain. Eur J Neurosci 51, 268–281. [PubMed: 30059181]
14. Leiserson WM, Forbush B, and Keshishian H (2010). Drosophila glia use a conserved cotransporter mechanism to regulate extracellular volume. Glia 59, 320–332.
15. Sun Q, Tian E, Turner RJ, and Hagen KGT (2009). Developmental and functional studies of the SLC12 gene family members from Drosophila melanogaster. Am J Physiology Cell Physiology 298, C26–37.
16. Rodan AR, Baum M, and Huang C-L (2012). The Drosophila NKCC Ncc69 is required for normal renal tubule function. Am J Physiol-cell Ph 303, C883–C894.
17. Arosio D, Ricci F, Marchetti L, Gualdani R, Albertazzi L, and Beltram F (2010). Simultaneous intracellular chloride and pH measurements using a GFP-based sensor. Nat Methods 7, 516–8. [PubMed: 20581829]
18. Mukhtarov M, Liguori L, Waseem T, Rocca F, Buldakova S, Arosio D, and Bregestovski P (2013). Calibration and functional analysis of three genetically encoded Cl−/pH sensors. Front Mol Neurosci 6, 9. [PubMed: 23616745]
19. Sun Q, Wu Y, Jonusaite S, Pleinis JM, Humphreys JM, He H, Schellinger JN, Akella R, Stenesen D, Krämer H, et al. (2018). Intracellular Chloride and Scaffold Protein Mo25 Cooperatively Regulate Transepithelial Ion Transport through WNK Signaling in the Malpighian Tubule. J Am Soc Nephrol 29, 1449–1461. [PubMed: 29602832]
20. Pleinis JM, Norrell L, Akella R, Humphreys JM, He H, Sun Q, Zhang F, Sosa-Pagan J, Morrison DE, Schellinger JN, et al. (2021). WNKs are potassium-sensitive kinases. Am J Physiol-cell Ph 320, C703–C721.
21. Stoleru D, Peng Y, Agosto J, and Rosbash M (2004). Coupled oscillators control morning and evening locomotor behaviour of Drosophila. Nature 431, 862–868. [PubMed: 15483615]
22. Grima B, Chélot E, Xia R, and Rouyer F (2004). Morning and evening peaks of activity rely on different clock neurons of the Drosophila brain. Nature 431, 869–873. [PubMed: 15483616]
23. Guo F, Cerullo I, Chen X, and Rosbash M (2014). PDF neuron firing phase-shifts key circadian activity neurons in Drosophila. Elife 3, e02780.

24. Renn SCP, Park JH, Rosbash M, Hall JC, and Taghert PH (1999). A pdf Neuropeptide Gene Mutation and Ablation of PDF Neurons Each Cause Severe Abnormalities of Behavioral Circadian Rhythms in Drosophila. Cell 99, 791–802. [PubMed: 10619432]
25. Yao Z, and Shafer OT (2014). The Drosophila Circadian Clock Is a Variably Coupled Network of Multiple Peptidergic Units. Science 343, 1516–1520. [PubMed: 24675961]
26. Nitabach MN, and Taghert PH (2008). Organization of the Drosophila circadian control circuit. Curr Biology Cb 18, R84–93.
27. Parisky KM, Agosto J, Pulver SR, Shang Y, Kuklin E, Hodge JJL, Kang K, Kang K, Liu X, Garrity PA, et al. (2008). PDF Cells Are a GABA-Responsive Wake-Promoting Component of the Drosophila Sleep Circuit. Neuron 60, 672–682. [PubMed: 19038223]
28. Chung BY, Kilman VL, Keath JR, Pitman JL, and Allada R (2009). The GABAA Receptor RDL Acts in Peptidergic PDF Neurons to Promote Sleep in Drosophila. Curr Biol 19, 386–390. [PubMed: 19230663]
29. Park JH, Helfrich-Forster C, Lee G, Liu L, Rosbash M, and Hall JC (2000). Differential regulation of circadian pacemaker output by separate clock genes in Drosophila. Proc National Acad Sci 97, 3608–3613.
30. Rusan ZM, Kingsford OA, and Tanouye MA (2014). Modeling Glial Contributions to Seizures and Epileptogenesis: Cation-Chloride Cotransporters in Drosophila melanogaster. Plos One 9, e101117. [PubMed: 24971529]
31. Stenesen D, Moehlman AT, Schellinger JN, Rodan AR, and Krämer H (2019). The glial sodium-potassium-2-chloride cotransporter is required for synaptic transmission in the Drosophila visual system. Sci Rep-uk 9, 2475.
32. Ng FS, Sengupta S, Huang Y, Yu AM, You S, Roberts MA, Iyer LK, Yang Y, and Jackson FR (2016). TRAP-seq Profiling and RNAi-Based Genetic Screens Identify Conserved Glial Genes Required for Adult Drosophila Behavior. Front Mol Neurosci 9, 146. [PubMed: 28066175]
33. Alessi DR, Zhang J, Khanna A, Hochdorfer T, Shang Y, and Kahle KT (2014). The WNK-SPAK/OSR1 pathway: Master regulator of cation-chloride cotransporters. Sci Signal 7, re3–re3. [PubMed: 25028718]
34. Rodan AR (2018). WNK-SPAK/OSR1 signaling: lessons learned from an insect renal epithelium. Am J Physiology Ren Physiology 315, F903–F907.
35. Piala AT, Moon TM, Akella R, He H, Cobb MH, and Goldsmith EJ (2014). Chloride Sensing by WNK1 Involves Inhibition of Autophosphorylation. Sci Signal 7, ra41–ra41. [PubMed: 24803536]
36. Terker AS, Zhang C, Erspamer KJ, Gamba G, Yang C-L, and Ellison DH (2016). Unique chloride-sensing properties of WNK4 permit the distal nephron to modulate potassium homeostasis. Kidney Int 89, 127–134. [PubMed: 26422504]
37. Vitari AC, Deak M, Morrice NA, and Alessi DR (2005). The WNK1 and WNK4 protein kinases that are mutated in Gordon's hypertension syndrome phosphorylate and activate SPAK and OSR1 protein kinases. Biochem J 391, 17–24. [PubMed: 16083423]
38. Anselmo AN, Earnest S, Chen W, Juang Y-C, Kim SC, Zhao Y, and Cobb MH (2006). WNK1 and OSR1 regulate the Na+, K+, 2Cl− cotransporter in HeLa cells. Proc National Acad Sci 103, 10883–10888.
39. Wu Y, Schellinger JN, Huang C-L, and Rodan AR (2014). Hypotonicity Stimulates Potassium Flux through the WNK-SPAK/OSR1 Kinase Cascade and the Ncc69 Sodium-Potassium-2-Chloride Cotransporter in the Drosophila Renal Tubule. J Biol Chem 289, 26131–26142. [PubMed: 25086033]
40. Delpire E, and Gagnon KBE (2007). Genome-wide analysis of SPAK/OSR1 binding motifs. Physiol Genomics 28, 223–231. [PubMed: 17032814]
41. Ruben M, Drapeau MD, Mizrak D, and Blau J (2012). A Mechanism for Circadian Control of Pacemaker Neuron Excitability. J Biol Rhythm 27, 353–364.
42. Kula-Eversole E, Nagoshi E, Shang Y, Rodriguez J, Allada R, and Rosbash M (2010). Surprising gene expression patterns within and between PDF-containing circadian neurons in Drosophila. P Natl Acad Sci Usa 107, 13497–502.

43. Huang Y, Ainsley JA, Reijmers LG, and Jackson FR (2013). Translational Profiling of Clock Cells Reveals Circadianly Synchronized Protein Synthesis. Plos Biol 11, e1001703. [PubMed: 24348200]
44. Taylor CA, An S-W, Kankanamalage SG, Stippec S, Earnest S, Trivedi AT, Yang JZ, Mirzaei H, Huang C-L, and Cobb MH (2018). OSR1 regulates a subset of inward rectifier potassium channels via a binding motif variant. P Natl Acad Sci Usa 115, 3840–3845.
45. Cherbas L, Willingham A, Zhang D, Yang L, Zou Y, Eads BD, Carlson JW, Landolin JM, Kapranov P, Dumais J, et al. (2011). The transcriptional diversity of 25 Drosophila cell lines. Genome Res 21, 301–314. [PubMed: 21177962]
46. Wu Y, Baum M, Huang C-L, and Rodan AR (2015). Two inwardly rectifying potassium channels, Irk1 and Irk2, play redundant roles in Drosophila renal tubule function. Am J Physiology-regulatory Integr Comp Physiology 309, R747–R756.
47. Hong S-T, Bang S, Paik D, Kang J, Hwang S, Jeon K, Chun B, Hyun S, Lee Y, and Kim J (2006). Histamine and Its Receptors Modulate Temperature-Preference Behaviors in Drosophila. J Neurosci 26, 7245–7256. [PubMed: 16822982]
48. Dahdal D, Reeves DC, Ruben M, Akabas MH, and Blau J (2010). Drosophila Pacemaker Neurons Require G Protein Signaling and GABAergic Inputs to Generate Twenty-Four Hour Behavioral Rhythms. Neuron 68, 964–977. [PubMed: 21145008]
49. Collins B, Kaplan HS, Cavey M, Lelito KR, Bahle AH, Zhu Z, Macara AM, Roman G, Shafer OT, and Blau J (2014). Differentially Timed Extracellular Signals Synchronize Pacemaker Neuron Clocks. Plos Biol 12, e1001959. [PubMed: 25268747]
50. Lüscher BP, Vachel L, Ohana E, and Muallem S (2020). Cl− as a bona fide signaling ion. Am J Physiol-cell Ph 318, C125–C136.
51. Rodan AR (2019). Intracellular chloride: a regulator of transepithelial transport in the distal nephron. Curr Opin Nephrol Hy 28, 360–367.
52. Terker AS, Zhang C, McCormick JA, Lazelle RA, Zhang C, Meermeier NP, Siler DA, Park HJ, Fu Y, Cohen DM, et al. (2015). Potassium Modulates Electrolyte Balance and Blood Pressure through Effects on Distal Cell Voltage and Chloride. Cell Metab 21, 39–50. [PubMed: 25565204]
53. Chen J-C, Lo Y-F, Lin Y-W, Lin S-H, Huang C-L, and Cheng C-J (2019). WNK4 kinase is a physiological intracellular chloride sensor. Proc National Acad Sci 116, 4502–4507.
54. Perry JSA, Morioka S, Medina CB, Etchegaray JI, Barron B, Raymond MH, Lucas CD, Onengut-Gumuscu S, Delpire E, and Ravichandran KS (2019). Interpreting an apoptotic corpse as anti-inflammatory involves a chloride sensing pathway. Nat Cell Biol 21, 1532–1543. [PubMed: 31792382]
55. Buhl E, Bradlaugh A, Ogueta M, Chen K-F, Stanewsky R, and Hodge JJL (2016). Quasimodo mediates daily and acute light effects on Drosophila clock neuron excitability. Proc National Acad Sci 113, 13486–13491.
56. Piermarini PM, Akuma DC, Crow JC, Jamil TL, Kerkhoff WG, Viel KCMF, and Gillen CM (2017). Differential expression of putative sodium-dependent cation-chloride cotransporters in Aedes aegypti. Comp Biochem Physiology Part Mol Integr Physiology 214, 40–49.
57. Kalsi M, Gillen C, and Piermarini P (2019). Heterologous Expression of Aedes aegypti Cation Chloride Cotransporter 2 (aeCCC2) in Xenopus laevis Oocytes Induces an Enigmatic Na+/Li+ Conductance. Insects 10, 71.
58. Jeu M. de, Hermes M, and Pennartz C (1998). Circadian modulation of membrane properties in slices of rat suprachiasmatic nucleus. Neuroreport 9, 3725–3729. [PubMed: 9858386]
59. Michel S, Geusz M, Zaritsky J, and Block G (1993). Circadian rhythm in membrane conductance expressed in isolated neurons. Science 259, 239–241. [PubMed: 8421785]
60. Welsh DK, Logothetis DE, Meister M, and Reppert SM (1995). Individual neurons dissociated from rat suprachiasmatic nucleus express independently phased circadian firing rhythms. Neuron 14, 697–706. [PubMed: 7718233]
61. Nitabach MN, Blau J, and Holmes TC (2002). Electrical Silencing of Drosophila Pacemaker Neurons Stops the Free-Running Circadian Clock. Cell 109, 485–495. [PubMed: 12086605]
62. Wu Y, Cao G, and Nitabach MN (2008). Electrical silencing of PDF neurons advances the phase of non-PDF clock neurons in Drosophila. J Biol Rhythm 23, 117–28.

63. Mizrak D, Ruben M, Myers GN, Rhrissorrakrai K, Gunsalus KC, and Blau J (2012). Electrical activity can impose time of day on the circadian transcriptome of pacemaker neurons. Curr Biology Cb 22, 1871–80. [PubMed: 22940468]
64. Depetris-Chauvin A, Berni J, Aranovich EJ, Muraro NI, Beckwith EJ, and Ceriani MF (2011). Adult-Specific Electrical Silencing of Pacemaker Neurons Uncouples Molecular Clock from Circadian Outputs. Curr Biol 21, 1783–1793. [PubMed: 22018542]
65. Nitabach MN, Wu Y, Sheeba V, Lemon WC, Strumbos J, Zelensky PK, White BH, and Holmes TC (2006). Electrical Hyperexcitation of Lateral Ventral Pacemaker Neurons Desynchronizes Downstream Circadian Oscillators in the Fly Circadian Circuit and Induces Multiple Behavioral Periods. J Neurosci 26, 479–489. [PubMed: 16407545]
66. Smith P, Buhl E, Tsaneva-Atanasova K, and Hodge JJL (2019). Shaw and Shal voltage-gated potassium channels mediate circadian changes in Drosophila clock neuron excitability. J Physiology 597, 5707–5722.
67. Flourakis M, Kula-Eversole E, Hutchison AL, Han TH, Aranda K, Moose DL, White KP, Dinner AR, Lear BC, Ren D, et al. (2015). A Conserved Bicycle Model for Circadian Clock Control of Membrane Excitability. Cell 162, 836–48. [PubMed: 26276633]
68. Hibino H, Inanobe A, Furutani K, Murakami S, Findlay I, and Kurachi Y (2010). Inwardly Rectifying Potassium Channels: Their Structure, Function, and Physiological Roles. Physiol Rev 90, 291–366. [PubMed: 20086079]
69. Cao G, and Nitabach MN (2008). Circadian control of membrane excitability in Drosophila melanogaster lateral ventral clock neurons. J Neurosci Official J Soc Neurosci 28, 6493–501.
70. Zhuang J, Zhang X, Wang D, Li J, Zhou B, Shi Z, Gu D, Denson DD, Eaton DC, and Cai H (2011). WNK4 kinase inhibits Maxi K channel activity by a kinase-dependent mechanism. Am J Physiol-renal 301, F410–F419.
71. Yue P, Zhang C, Lin D-H, Sun P, and Wang W-H (2013). WNK4 inhibits Ca(2+)-activated big-conductance potassium channels (BK) via mitogen-activated protein kinase-dependent pathway. Biochim Biophys Acta 1833, 2101–10. [PubMed: 23673010]
72. Wang Z, Subramanya AR, Satlin LM, Pastor-Soler NM, Carattino MD, and Kleyman TR (2013). Regulation of large-conductance Ca 2+ -activated K + channels by WNK4 kinase. Am J Physiol-cell Ph 305, C846–C853.
73. Webb TN, Carrisoza-Gaytan R, Montalbetti N, Rued A, Roy A, Socovich AM, Subramanya AR, Satlin LM, Kleyman TR, and Carattino MD (2016). Cell-specific regulation of L-WNK1 by dietary K +. Am J Physiol-renal 310, F15–F26.
74. Liu Y, Song X, Shi Y, Shi Z, Niu W, Feng X, Gu D, Bao H-F, Ma H-P, Eaton DC, et al. (2014). WNK1 activates large-conductance Ca2+-activated K+ channels through modulation of ERK1/2 signaling. J Am Soc Nephrol Jasn 26, 844–54. [PubMed: 25145935]
75. Ray EC, Carrisoza-Gaytán R, Al-bataineh MM, Marciszyn AL, Nkashama LJ, Chen J, Winfrey A, Griffiths SE, Lam T, Flores D, et al. (2021). L-WNK1 is required for BK channel activation in intercalated cells. Am J Physiol-renal.
76. Lee H, McManus CJ, Cho D-Y, Eaton M, Renda F, Somma MP, Cherbas L, May G, Powell S, Zhang D, et al. (2014). DNA copy number evolution in Drosophila cell lines. Genome Biol 15, R70. [PubMed: 25262759]
77. Bischof J, Maeda RK, Hediger M, Karch F, and Basler K (2007). An optimized transgenesis system for Drosophila using germ-line-specific C31 integrases. Proc National Acad Sci 104, 3312–3317.
78. Schlichting M, Díaz MM, Xin J, and Rosbash M (2019). Neuron-specific knockouts indicate the importance of network communication to Drosophila rhythmicity. Elife 8, e48301. [PubMed: 31613223]
79. Cyran SA, Yiannoulos G, Buchsbaum AM, Saez L, Young MW, and Blau J (2005). The Double-Time Protein Kinase Regulates the Subcellular Localization of the Drosophila Clock Protein Period. J Neurosci 25, 5430–5437. [PubMed: 15930393]
80. Wang JW, Wong AM, Flores J, Vosshall LB, and Axel R (2003). Two-Photon Calcium Imaging Reveals an Odor-Evoked Map of Activity in the Fly Brain. Cell 112, 271–282. [PubMed: 12553914]

81. Piechotta K, Lu J, and Delpire E (2002). Cation Chloride Cotransporters Interact with the Stress-related Kinases Ste20-related Proline-Alanine-rich Kinase (SPAK) and Oxidative Stress Response 1 (OSR1). J Biol Chem 277, 50812–50819. [PubMed: 12386165]

82. Heros P. de los, Alessi DR, Gourlay R, Campbell DG, Deak M, Macartney TJ, Kahle KT, and Zhang J (2014). The WNK-regulated SPAK/OSR1 kinases directly phosphorylate and inhibit the K+–Cl− co-transporters. Biochem J 458, 559–573. [PubMed: 24393035]

83. Zhang J, Gao G, Begum G, Wang J, Khanna AR, Shmukler BE, Daubner GM, Heros P. de L., Davies P, Varghese J, et al. (2016). Functional kinomics establishes a critical node of volume-sensitive cation-Cl(−) cotransporter regulation in the mammalian brain. Sci Rep-uk 6, 35986.

84. Melo Z, Heros P. de los, Cruz-Rangel S, Vázquez N, Bobadilla NA, Pasantes-Morales H, Alessi DR, Mercado A, and Gamba G (2013). N-terminal serine dephosphorylation is required for KCC3 cotransporter full activation by cell swelling. J Biological Chem 288, 31468–76.

85. González M, Martín-Ruíz I, Jiménez S, Pirone L, Barrio R, and Sutherland JD (2011). Generation of stable Drosophila cell lines using multicistronic vectors. Sci Rep-uk 1, 75.

86. Hekmat-Scafe DS, Lunday MY, Ranga R, and Tanouye MA (2006). Mutations in the K+/Cl− cotransporter gene kazachoc (kcc) increase seizure susceptibility in Drosophila. J Neurosci 35, 8943–8954

Highlights.

- Intracellular chloride oscillates in *Drosophila* sLN_v pacemaker neurons.
- The morning increase in chloride restrains activity of the WNK-Fray kinase cascade
- Fray activates an inwardly rectifying potassium channel, Irk1
- Chloride inhibition of the WNK-Fray-Irk1 pathway maintains normal circadian period

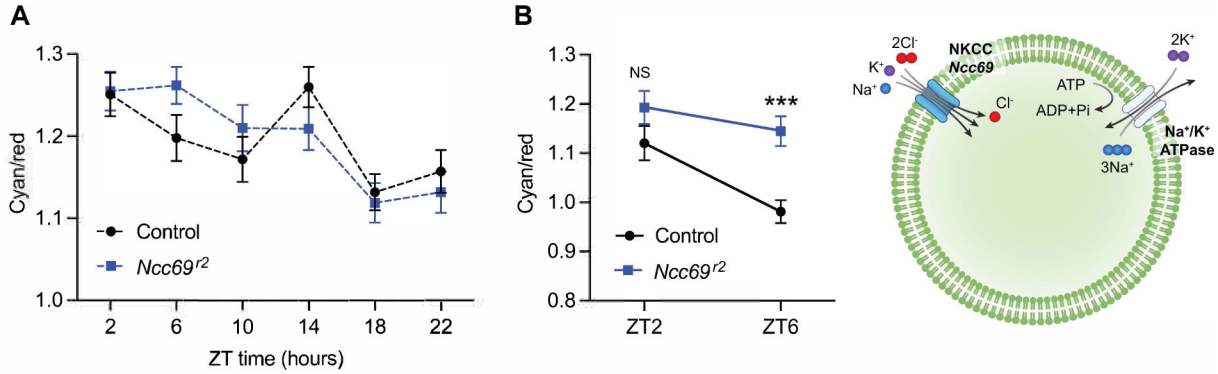

Figure 1. Intracellular chloride increases in sLN$_v$ pacemakers during the morning in an NKCC-dependent manner

A) Cyan/red ratios, which are the inverse of intracellular chloride concentrations (Figure S1), were measured using the transgenic sensor ClopHensor. The cyan/red ratios vary over time in sLN$_v$ pacemaker neurons. Mean ± SEM shown. ZT0, lights on. $p<0.0001$ for time, $p=0.8495$ for genotype, two-way ANOVA. Intracellular pH from the same neurons and numbers of neurons analyzed is shown in Table S1. Control and *Ncc69* mutant flies were analyzed in parallel, with different timepoints measured on different days. B) Cyan/red ratios, measured in the same sLN$_v$s over time, 2 and 6 hours after lights-on. Mean ± SEM shown. Table S2 lists genotypes and numbers of flies analyzed here and subsequently. Significant effects of time ($p=0.0004$) and genotype ($p=0.0042$), two-way repeated measures ANOVA. ***, $p=0.0010$ for cyan/red ratio in control vs. *Ncc69^{r2}* mutant, Šidák's multiple comparison test. ZT6 was significantly different from ZT2 in control ($p=0.0007$) but not *Ncc69^{r2}* mutants ($p=0.2577$), Šidák's multiple comparison test. NS, not significant.
See also Figure S1 and Tables S1–S2.

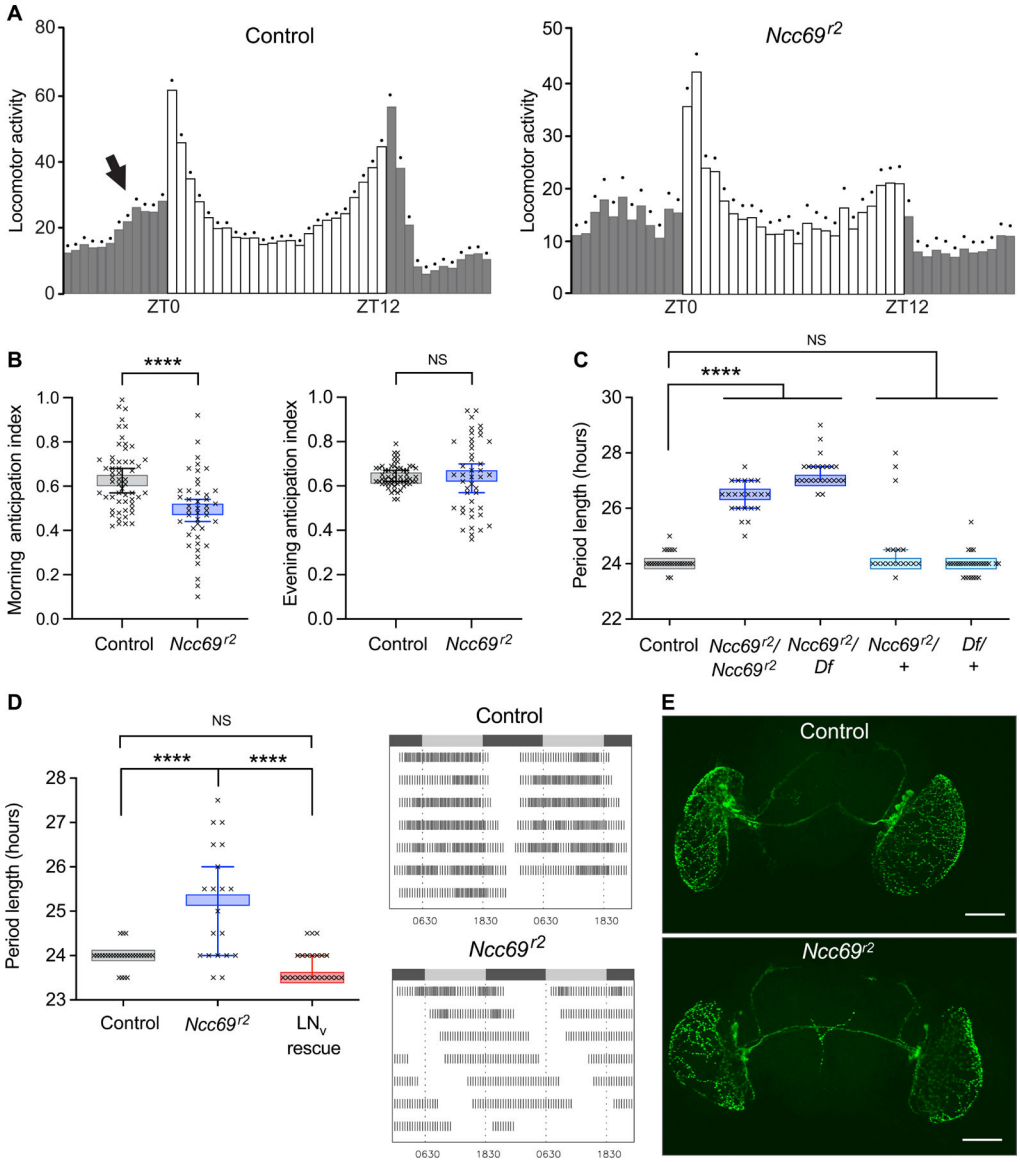

Figure 2. The *Ncc69* NKCC is required in sLN$_v$ pacemakers for normal circadian behavior

A) Actograms showing locomotor activity during lights off (grey bars) and lights on (white bars) in control and *Ncc69*^{r2} mutants. The arrow indicates increasing locomotor activity (morning anticipation) prior to lights on. Morning anticipation is abolished in *Ncc69*^{r2} mutants. Mean + SEM (dots) shown. B) Morning and evening anticipation index. An anticipation index of 0.5 (see Methods) indicates no anticipation, whereas a value of greater than 0.5 indicates anticipation. Median and 95th percentile confidence intervals graphed for behavioral data in this and subsequent figures, with individual data points shown. ****, p<0.0001; NS, not significant, unpaired t-test. C) Circadian period is prolonged in *Ncc69* mutants. Locomotor activity was measured in constant darkness for 7 days here and subsequently. ****, p<0.0001. Statistical tests used in C and D are listed in Table S3. D) Expression of wild-type *Ncc69* in the LN$_v$ pacemakers, under the control of *pdf*-GAL4, rescues the long-period phenotype of *Ncc69* mutant flies. ****, p<0.0001. Right,

representative actograms showing average activity across 7 days of subjective day (grey bars) and night (dark bars) in constant darkness. E) LN_v morphology is intact in *Ncc69* mutants. PDF neuropeptide-expressing pacemaker neurons were visualized using α-PDF antibodies. Immunostaining in *Ncc69* mutants and controls was performed in parallel. Scale bar, 100 μm.

See also Tables S2–S3.

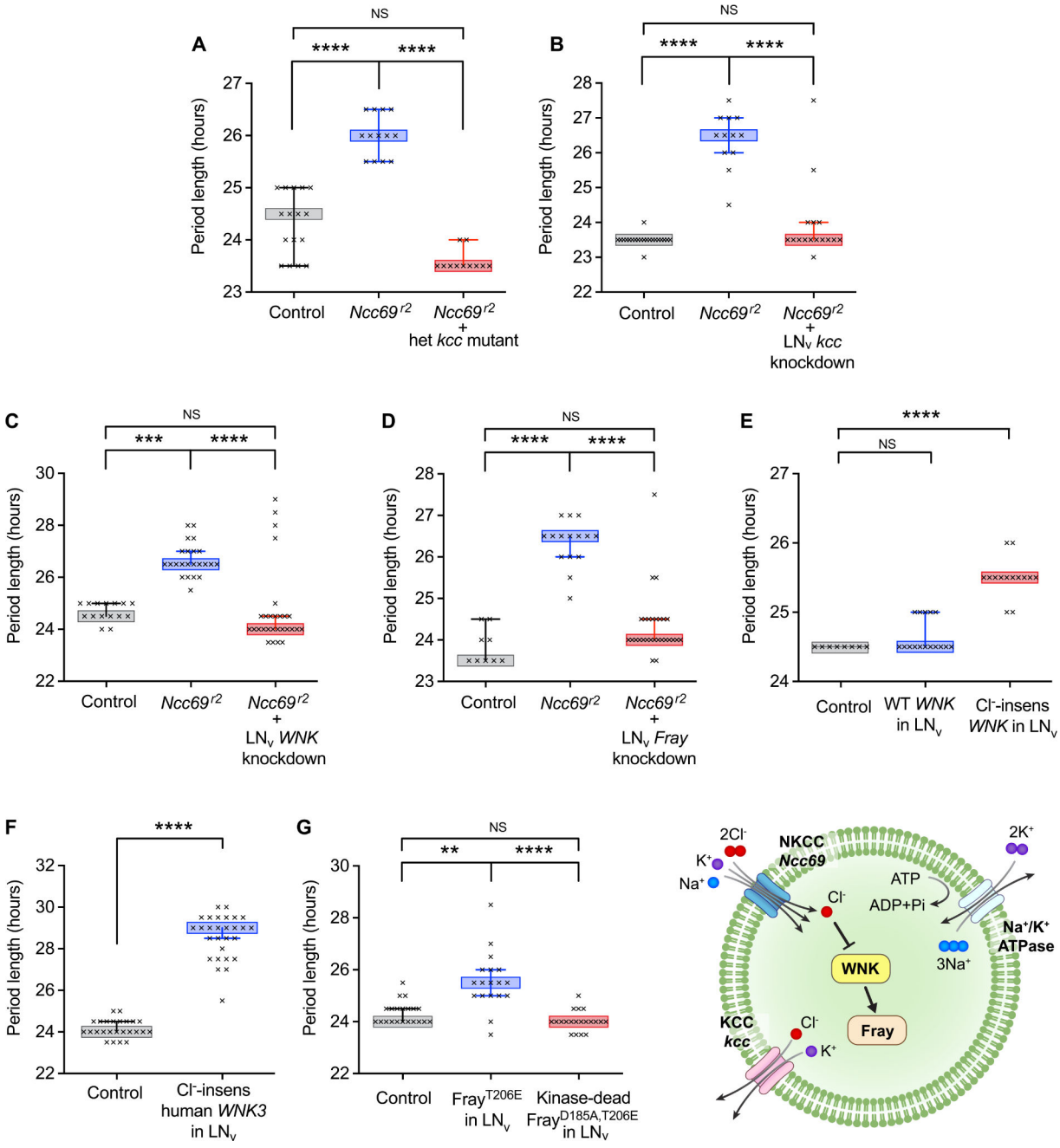

Figure 3. Period lengthening in *Ncc69* mutants is due to low chloride activation of the WNK-Fray kinase cascade.

Heterozygous loss of *kcc* (A) or knockdown of *kcc* in LN_v pacemakers (B) suppresses the long-period phenotype of *Ncc69* mutants. LN_v knockdown of the chloride-inhibited *WNK* kinase (C) or its downstream target, *Fray* (D), suppresses the long-period phenotype of *Ncc69* mutants. LN_v overexpression of Cl^--insensitive, but not wild-type, *Drosophila WNK* (E) or human WNK3 (F) results in lengthening of circadian period. G) Overexpression of activated $Fray^{T206E}$, but not kinase-dead $Fray^{D185A,T206E}$, increases period length. **, p=0.0026; ***, p=0.0007; ****, p<0.0001. See Table S3 for statistical tests used.

See also Tables S2–S4.

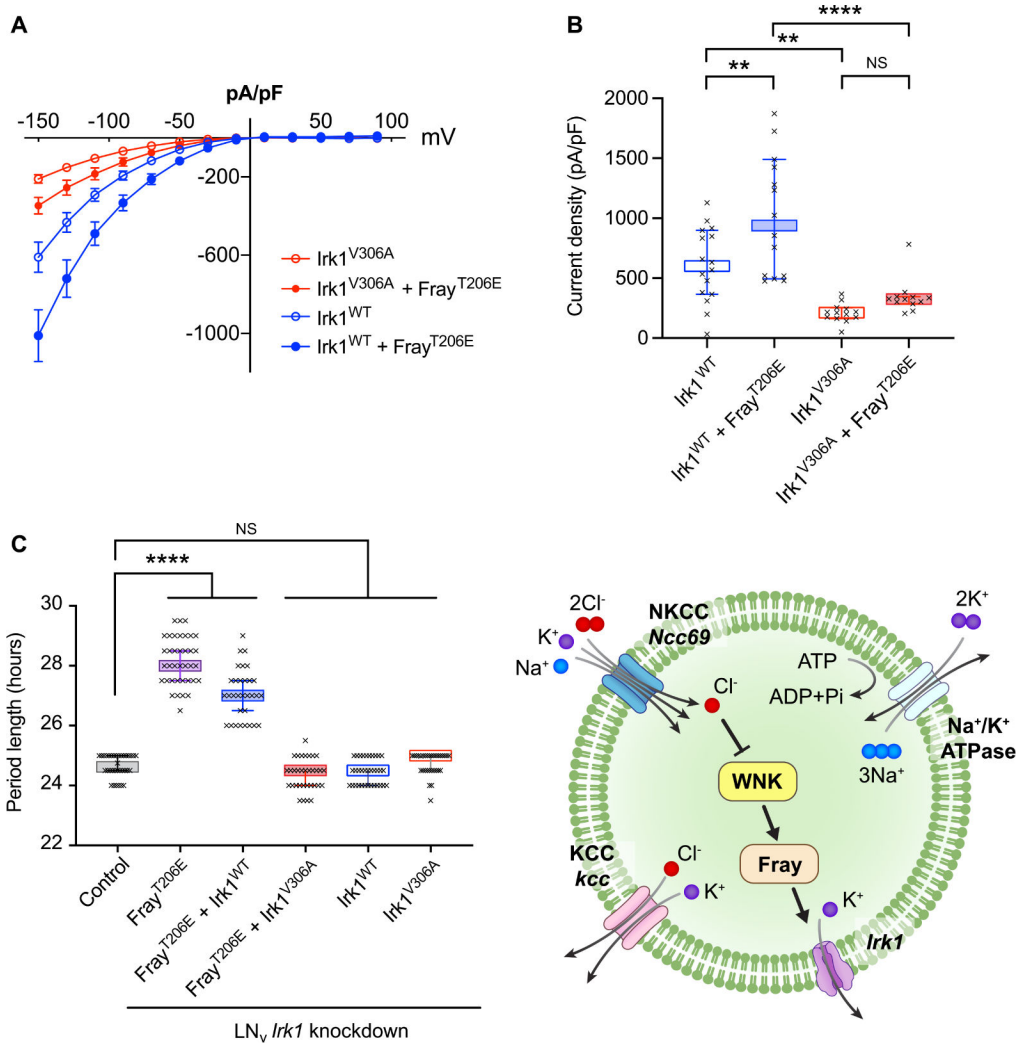

Figure 4. Fray activates the inwardly rectifying potassium channel Irk1 to prolong circadian period.

Fray^{T206E} expression increases activity of wild-type Irk1, but not Irk1^{V306A}, carrying a mutation in the predicted Fray-binding RFXV motif. A) Current-voltage curves from S2-R+ *Drosophila* cultured cells transfected with wild-type Irk1 or Irk1^{V306A}, with or without co-expression of constitutively active Fray^{T206E}. B) Current density at −150 mV. **, p<0.01, ****, p<0.0001, two-way ANOVA with Tukey's multiple comparisons test. n=12–16 cells analyzed/genotype. C) Irk1^{V306A} suppresses the long-period phenotype of Fray^{T206E}. *Irk1* was knocked down in the LN$_v$ pacemakers using RNAi, and replaced with *Irk1^{WT}* or *Irk1^{V306A}* transgenes with silent mutations in the RNAi target sites. ****, p<0.0001. See Table S3 for statistical tests used.

See also Table S2, S3, Data S1A and Figure S2.

Key resources table

REAGENT or RESOURCE	SOURCE	IDENTIFIER
Antibodies		
Mouse monoclonal anti-PDF C7 antibody	Developmental Studies Hybridoma Bank	Cat#PDF C7; RRID: AB_760350
Goat anti-mouse polyclonal IgG (H+L) cross-adsorbed secondary antibody, Alexa Fluor 488	Thermo Fisher	Cat#A-11001
Chemicals, peptides, and recombinant proteins		
CellFectin	Thermo Fisher	Cat#10362100
tributyltinchloride	Sigma	Cat#T50202
nigericin	Thermo Fisher	Cat#N1495
carbonyl cyanide 3-chlorophenylhydrazone	Sigma	Cat#C2759
valinomycin	Sigma	Cat#V0627
TransIT-Insect transfection reagent	Mirus Bio	Cat#6104
Critical commercial assays		
LR Clonase II	Thermo Fisher	Cat#11791020
Phusion high-fidelity DNA polymerase	New England Biolabs	Cat#M0530
QIAquick	Qiagen	Cat#28104
pENTR/D-TOPO cloning kit	Thermo Fisher	Cat#K240020
QuikChange II XL	Agilent	Cat#200521
NEBuilder HiFi DNA Assembly	New England Biolabs	Cat#E2621
Experimental models: Cell lines		
D. melanogaster: Cell line S2-R+	Krämer; *Drosophila* Genomics Resource Center	Cat#150; RRID:CVCL_Z831
Experimental models: Organisms/strains		
D. melanogaster: control: *wBerlin*	Rothenfluh	N/A
D. melanogaster: LN_v driver: *w; pdf*-GAL4	Rosbash[24]	N/A
D. melanogaster: Ncc69 mutant: *w; Ncc69*$^{-2}$	Leiserson[14]	N/A
D. melanogaster: Ncc69 rescue: *w; Ncc69*$^{-2}$ UAS-HA-Ncc69$^{2-3}$	Leiserson[14]	N/A
D. melanogaster: Glial *Ncc69* rescue: *w; gli*-GAL4; *Ncc69*$^{-2}$ UAS-HA-Ncc69$^{2-3}$	Leiserson[14]	N/A
D. melanogaster: kcc mutant: *w; kcc*^{DHS1}	Hekmat-Scafe[86]	N/A
D. melanogaster: RNAi targeting *kcc*: *w;* UAS-kcc^{RNAi}	Vienna *Drosophila* Resource Center	ID 101742; RRID: FlyBase_FBst0473615
D. melanogaster: Ncc69 deficiency: *w*^{1118}*;Df(3L)ED4475, p{3'.RS5+3.3'}ED4475/TM6C, cu*^{1} *Sb*^{1}	Bloomington *Drosophila* Stock Center	RRID: BDSC_8069
D. melanogaster: Dicer transgene: *w;* UAS-dcr-2	Bloomington *Drosophila* Stock Center	RRID: BDSC_24651
D. melanogaster: RNAi targeting *WNK*: *w;* UAS-WNK^{RNAi}	Bloomington *Drosophila* Stock Center; validated in [19]	RRID: BDSC_42521
D. melanogaster: RNAi targeting *WNK*: *w;* UAS-WNK^{RNAi} (Vienna)	Vienna *Drosophila* Resource Center; validated in [39]	ID 106928; RRID: FlyBase_FBst0478751
D. melanogaster: Wild-type WNK: *w;* UAS-WNK^{WT}	Rodan[19]	N/A

REAGENT or RESOURCE	SOURCE	IDENTIFIER
D. melanogaster: Chloride-insensitive WNK: *w;* UAS-WNK^{L421F}	Rodan[19]	N/A
D. melanogaster: Human WNK3: *w;* UAS-WNK3^{WT}	Rodan[31]	N/A
D. melanogaster: Chloride-insensitive human WNK3: *w;* UAS-WNK3^{L295F}	Rodan[20]	N/A
D. melanogaster: RNAi targeting *Fray*: *w*; UAS-fray^{RNAi}	Rodan[39]	N/A
D. melanogaster: RNAi targeting *Fray*: *w*; UAS-fray^{RNAi} (Vienna)	Vienna *Drosophila* Resource Center	ID 106919; RRID: FlyBase_FBst0478742
D. melanogaster: Activated Fray: *w;* UAS-Fray^{T206E}	Rodan[39]	N/A
D. melanogaster: Kinase-dead activated Fray: *w;* UAS-Fray^{D185A,T206E}	This paper	N/A
D. melanogaster: RNAi targeting *Irk1*: *w;* UAS-Irk1^{RNAi}	Bloomington *Drosophila* Stock Center; validated in [46]	RRID: BDSC_25823
D. melanogaster: WT Irk1 (RNAi-resistant): *w;* UAS-Irk1^{WT-RR}	This paper	N/A
D. melanogaster: V306A mutant Irk1 (RNAi-resistant): *w;* UAS-Irk1$^{V306A-RR}$	This paper	N/A
D. melanogaster: pH/chloride sensor: *w;* UAS-ClopHensor c202	Krämer[19]	N/A
D. melanogaster: injection strain for UAS-Fray^{D185A,T206E}: *y^{1}M{vas-int.Dm}ZH-2A w**; *M{3xP3-RFP.attP´}ZH-22A*	Bloomington *Drosophila* Stock Center	RRID: BDSC_24481
D. melanogaster: injection strain for UAS-Irk1^{WT-RR} and UAS-Irk1$^{V306A-RR}$: *M{vas-int.Dm}ZH-2A, M{3xP3-RFP.attP}ZH-51D*	Bloomington *Drosophila* Stock Center	RRID: BDSC_24483
Oligonucleotides		
See Table S6	N/A	N/A
Recombinant DNA		
Fray^{D185A,T206E} ORF in Gateway donor plasmid: pENTR-Fray^{D185A,T206E}	Rodan[39]	N/A
Gateway destination vector: pUASg.attB	Bischof and Basler[77]	N/A
Irk1 ORF: FI16807	*Drosophila* Genomics Resource Center	Cat#1644763; Flybase_FBcl0742744
Gateway donor plasmid: pENTR	Thermo Fisher	Cat#K240020
Irk1^{WT} ORF in Gateway donor plasmid: pENTR-Irk1^{WT}	This paper	N/A
Irk1^{V306A} ORF in Gateway donor plasmid: pENTR-Irk1^{V306A}	This paper	N/A
RNAi-resistant Irk1^{WT} ORF in Gateway donor plasmid: pENTR-Irk1^{WT-RR}	This paper	N/A
RNAi-resistant Irk1^{V306A} ORF in Gateway donor plasmid: pENTR-Irk1$^{V306A-RR}$	This paper	N/A
RNAi-resistant Irk1^{WT} in pUAS plasmid: pUASg.attB-Irk1^{WT-RR}	This paper	N/A
RNAi-resistant Irk1^{V306A} in pUAS plasmid: pUASg.attB-Irk1$^{V306A-RR}$	This paper	N/A
Source for ClopHensor cDNA: pcDNA3-ClopHensor	Addgene[17]	Cat#25938; RRID: Addgene_25938
pIB plasmid	Thermo Fisher	Cat#V802001
pH/chloride sensor in S2 cell expression plasmid: pIB-ClopHensor	This paper	N/A

REAGENT or RESOURCE	SOURCE	IDENTIFIER
pAc5 source plasmid: pAc5 STABLE2 Neo	Addgene[85]	Cat#32426; RRID: Addgene_32426
$Irk1^{WT}$ in S2 cell expression plasmid: pAc5-$Irk1^{WT}$	This paper	N/A
$Irk1^{V306A}$ in S2 cell expression plasmid: pAc5-$Irk1^{V306A}$	This paper	N/A
$Fray^{T206E}$ ORF in Gateway donor plasmid: pENTR-$Fray^{T206E}$	Rodan[39]	N/A
$Irk1^{WT}$ and $Fray^{T206E}$ in multi-cistronic S2 cell expression plasmid: pAc5-$Irk1^{WT}$-$Fray^{T206E}$	This paper	N/A
$Irk1^{V306A}$ and $Fray^{T206E}$ in multi-cistronic S2 cell expression plasmid: pAc5-$Irk1^{V306A}$-$Fray^{T206E}$	This paper	N/A
Software and algorithms		
Software: Fly activity analysis suite (FAASx)	Boudinot and Rouyer, https://neuropsi.cnrs.fr/en/departments/cnn/group-leader-francois-rouyer/	N/A
Software: ClockLab, version 6	Actimetrics	RRID: SCR_014309
Software: FIJI	Image J, NIH, https://fiji.sc/	RRID: SCR_002285
Software: GraphPad Prism, version 9	GraphPad	RRID: SCR_002798
Software: Pulse	Molecular Devices	N/A
Software: pClamp, version 9.2	Molecular Devices	RRID: SCR_011323
Other		
DAM2 *Drosophila* activity monitors	Trikinetics	N/A
35 mm glass bottom dishes with 14 mm microwell/#1.5 cover glass	CellVis	Cat#D35-14-1.5-N
NCBI protein database	https://www.ncbi.nlm.nih.gov/protein/	RRID:SCR_003257